Frontiers in Heat and Mass Transfer (FHMT), 18, 15 (2022)
DOI: 10.5098/hmt.18.15

Global Digital Central
ISSN: 2151-8629

Frontiers in Heat and Mass Transfer

Available at www.ThermalFluidsCentral.org

NUMERICAL STUDY OF JET IMPINGEMENT FORCE AND HEAT TRANSFER ON A MOVING CURVED SURFACE

Ali Chitsazan[a], Georg Klepp[a], Birgit Glasmacher[b]

[a]*Institute for Energy Research, Ostwestfalen-Lippe University of Applied Sciences and Arts, Lemgo 32657, Germany*
[b]*Institute for Multiphase Processes, Leibniz University Hannover, Hannover 30167, Germany*

ABSTRACT

The effect of surface curvature, number of jets, number of jet rows, jet arrangement, crossflow, and surface motion on the heat transfer and pressure force performance from multiple impinging round jets on the moving flat and curved surface have been numerically evaluated. The more number of jets (more than three jets) has no significant effect on the average heat transfer rate. The more number of jet rows increases the strength of wall jets interference and crossflow effects and degrade the average heat transfer rates. There is a minor difference between inline and staggered arrangements on both moving flat and curved surfaces. The surface motion has a stronger effect on the impinging jets in the intermediate crossflow scheme than in the minimum crossflow scheme. The total average Nu on both moving flat and curved surfaces reduces with an increase in the velocity ratio and surface curvature. The pressure force is relatively insensitive to the surface motion on both moving flat and curved surfaces.

Keywords: Multiple jet rows, Heat transfer, Pressure force, Surface motion, Curvature.

1. INTRODUCTION

Jet impingements enhance the heat transfer rate in many industrial applications such as cooling, heating, and drying due to the large amounts of heat and mass transfer between the surface and the working fluid. Jet impingement flow has many applications in the industry such as the cooling of electronic and turbine components, drying of textile and paper, etc.

Fenot et al. (2008) found that increasing the curvature causes a small growth of Nu number in the impingement region and the curvature produces confinement of the jet flow that decreases the Nu number distribution. Harrington et al. (2017) observed that the very small relative curvature (d/D=0.016) did not cause any significant changes in either the flow distribution or the heat transfer level compared to the flat target surface. Patil and Vedula (2018) observed that the smaller curvature ratios have better performance on the local heat transfer coefficient. Li and Corder (2008) showed that the dual impinging jets (two jets close to each other) on the curved surface generally produce two high heat transfer regions in the stagnation point, and the peak value is slightly higher than a single jet with the same Re number. Patil and Vedula (2015) found that the peak Nu values with a single row and two rows of jet impinging on a concave surface are the same at H/d=2 and peak Nu values for the two-row case is higher than the single row case at H/d=4 despite the reduced impingement pressure due to the entrainment of the incoming jet. The inline and staggered patterns result in the same average Nu number. Bu et al. (2015) observed two peaks in the local Nu number distribution in the chordwise direction for two rows of jet holes due to the weak interference between adjacent air jets and only one peak for three rows of jet holes due to strong interference between adjacent air jets.

Some industrial processes such as paper dryer or rolling of sheet stock or external heat transfer to rotating parts require the target surface to move. The selection of an effective speed depends on several factors such as the jet spacing and a time constant associated with the heat and mass transfer rate to or from the target surface. For a small surface to jet velocity ratio up to 0.2, the surface motion has a negligible effect. When the surface velocity is higher, the effect is like that of superposing a crossflow (Zuckerma and Lior, 2006). Chattopadhyay (2006) found that the surface velocity affects strongly the flow field over the target surface and reduces the heat transfer rate. Kadiyala and Chattopadhyay (2017) observed that by increasing the surface velocities the heat transfer reduces initially and reaches a minimum and increases again. Maximum heat transfer is achieved for the stationary surface before transition, while the maximum heat transfer after transition is achieved at the velocity ratio equal to 6.

Obot and Trabold (1987) established that the best heat transfer performance with regard to the magnitude and uniformity occurs with the minimum crossflow scheme. Xing et al. (2010) concluded that if there is no dependence on the jet to plate spacings or crossflow, the inline configuration outperforms the staggered pattern. Wae-Hayee et al. (2013) found that the crossflow has a stronger effect on the impinging jets in the staggered pattern than in the in-line pattern.

Chitsazan et al. (2020) conducted a numerical investigation of jet impingement heat transfer and force on a moving flat surface for different jet Re numbers, nozzle to surface distance, jet to jet spacing, jet exit angle, and surface velocity.

It can be concluded that the above works focus on the orthogonal jets impinging on either the fixed curved surface or moving flat surface and there is not observed any investigation concerning the effect of orthogonal jets impinging on the moving curved surface. The heat transfer between multiple jets and a moving curved surface is more difficult to study due to the changing boundaries and effect of surface curvature but is also very relevant in engineering applications such as the drying process. The scope of this research is to investigate numerically the effect of surface curvature, number of jets, number of jet rows, jet arrangement (inline and staggered), cross-flow and surface motion on the heat transfer and pressure force from multiple impinging round jets on the moving flat and curved surface. This work contributes to a better understanding of the jet impingement heat transfer and pressure force on a moving curved surface, which can lead to the optimal design of the industrial drying system.

Global Digital Central
ISSN: 2151-8629

2. MATERIAL AND METHOD

2.1 Definition of Characteristic Numbers

The local heat transfer coefficient is nondimensionalized to the Nusselt number by the following expression:

$$Nu = \frac{hd}{k} = \frac{q}{(T_w - T_j)} . \frac{d}{k_t} \quad (1)$$

Where q is the convective heat flux, T_w is the target wall temperature, T_j is the jet exit temperature, d is the jet exit diameter, k_t is the thermal conductivity of the air at jet exit temperature and h is the local heat transfer coefficient.

Pressure force on the surface is the force that the fluid exerts in the direction of normal to the surface. Jet impingement force is presented in dimensionless form by a force coefficient C_f and defined as follows:

$$C_f = \frac{F}{0.5\rho V^2(\pi d^2/4)} \quad (2)$$

Where F is the pressure force on the surface, ρ is the density of the jet flow, d is the jet exit diameter and V is the jet exit velocity. The pressure force on the surface is computed as:

$$F = P_{st} A \quad (3)$$

Where P_{st} is the pressure at the stagnation point and A is the surface area.

2.2 Domain and Boundary Condition

Figure 1 shows the geometry of the multiple impinging jets and boundary conditions used. All jet inlets were modeled as circular planes in the top wall. The incoming jet flow is assumed to be with constant fluid properties at T_j = 298.15 K, entered with a uniform velocity profile. For all configurations, the pattern was regular. The target surface as a moving curved surface was modeled as a no-slip wall held at a constant temperature of T_w = 333.15 K. No-slip with adiabatic wall boundary conditions is imposed on all other solid surfaces. Constant pressure outlet boundary condition is applied to all open boundaries. The movement of the curved surface is considered along curvilinear axes. Symmetric boundary condition was also applied in the X-Y plane for the central jet to reduce the computational cost.

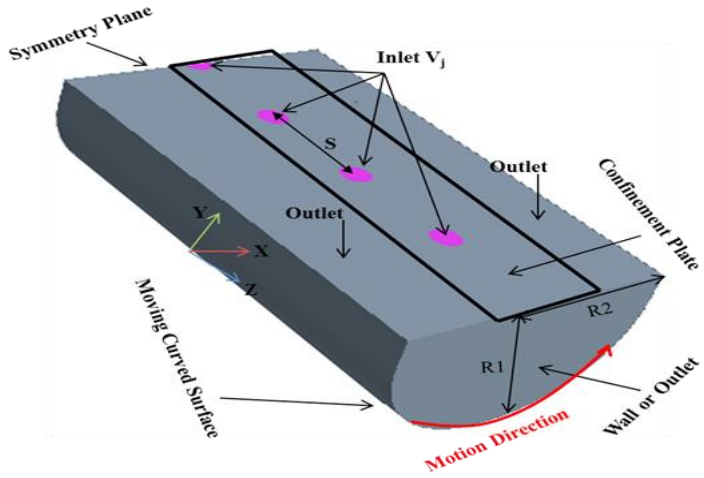

Fig. 1 Schematic of the computational domain

For industrial dryers; the variation of relative surface curvature (Cr) is brought by varying the minor radius (R1) between 0-40mm and the major radius of the impingement surface (R2) between 50-200 mm. The relative surface curvature (Cr) is defined as the ratio of minor radius (R1) to the major radius (R2). The data for different relative curvatures of 0.0 (flat surface), 0.2, 0.4, 0.6, 0.8, and 1 are brought by varying the minor radius (R1) and maintaining the major radius (R2=50mm). Details of the parameters investigated are presented in Table 1.

Table 1 Parameters investigated for a real industrial dryer

Parameters	Values
Number of jet rows	1, 3
Number of jets in an row	3, 5, 7, 13, 25, 49
Jet diameter (d)	10mm
Minor curvature radius(R_1)	0-40mm
Major curvature radius (R_2)	50mm
Inlet Jet temperature	25º C
Surface temperature	60º C
Surface velocity	0, 0.17, 1.7, 10 (m/s)
Jet angle (θ)	90 (°)
Jet Reynolds number (Re)	23000
Relative nozzle to plate distances (H/d)	2, 5
Relative nozzle to nozzle spacing (S/d)	2, 4
Relative surface curvature (Cr)	0, 0.2, 0.4, 0.6, 0.8, 1
Relative velocity ratio (VR)	0, 0.0047, 0.047, 0.28

2.3 Computational Detail

The CFD model is set up and run with the commercial code STAR-CCM+ 13.02.013. The final solution was obtained by applying a second-order discretization upwind scheme, and the SIMPLE algorithm is used for pressure-velocity coupling. SST k-ω turbulence model is used as recommended by many researchers (Xing et al., 2010; Wae-hayee et al. 2013). The flow in the near-wall regime was simulated using a low-Reynolds number approach. The solution was considered to be converged when the value of the scaled residual of the continuity, momentum, and energy equations is less than 10^{-4}.

2.4 Grid Generation and Sensitivity

An unstructured polyhedral grid was generated using STAR-CCM$^+$. A boundary layer with a dimensionless wall distance of less than one was built on the target surface. The grid was refined near the target surface to enable better resolution of the flow in this part.

The grid sensitivity study is carried out by analyzing the variation of the local Nu distribution on the target surface along the Z-centerline (the lines pass through the stagnation points of jets). The local discretization error distribution is calculated by applying the GCI method (Roache, 2003). The overall discretization error for the fine and intermediate grid (2.6 and 4.12% respectively) was very small. The intermediate grid is selected as the final grid to reduce the computational cost (see Table 2).

Table 2 Grid parameters of the refinement study at Re =23,000

Grid	Base Size (m)	Cell Number	Max y_1^+	Average GCI %
Course	0.00192	447,431	0.44	---
Intermediate	0.00127	970,045	0.31	4.12
Fine	0.00088	2,157,431	0.23	2.6

Global Digital Central
ISSN: 2151-8629

3. RESULTS AND DISCUSSION

3.1 Validation of CFD Simulation

Figure 2 indicates the local Nu along the curvilinear axis on the target surface. The numerical results of this work have been compared with the experimental data of Fenot (2008). The agreement between the two is very good and closely followed the same trend.

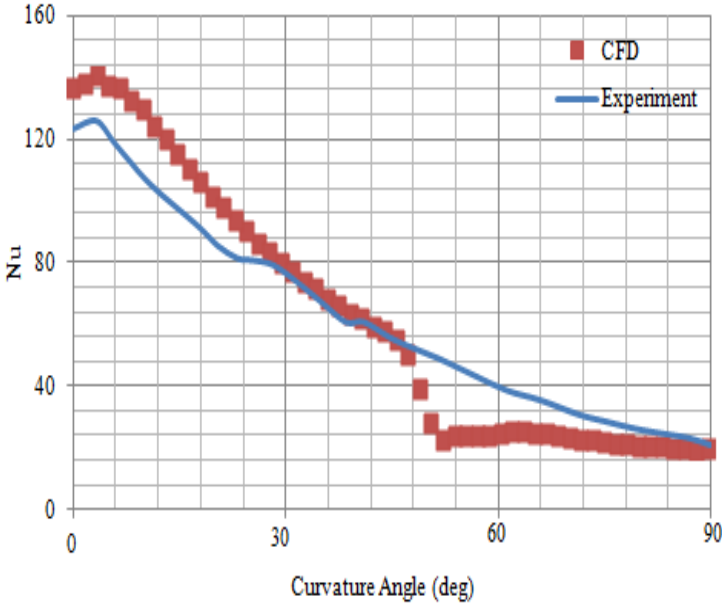

Fig. 2 Comparison of the local Nu along the curvilinear axis on a fixed curved surface between experiment and CFD (H/d=5, S/d=4, Re = 23000, Cr=1 and VR=0)

3.2 Surface Curvature

Since the relative curvature mainly influences the distributions along the curvilinear axis, Nusselt number distributions along curvilinear are the clearest way to observe its effects. Fig. 3 compares the effect of relative curvature on the local Nu distributions along the curvilinear axis on the target plate. Reducing the relative surface curvature allows impinging jets to make better contact with the surface and the Nusselt number distributions become much fatter than that of higher relative curvature and the lower relative curvature has more uniform heat transfer along the target surface. It can be concluded that the outflow of spent fluid is impeded by the concave curvature and adversely affects the local heat transfer. That's why; the concavity of the impingement plate produces a sort of confinement.

Figure 4 compares the effect of relative curvature on the total average Nu number on the target plate. It can be concluded that for higher relative curvature (Cr) which has a higher minor radius (R1), the confinement effect reduces the average heat transfer. We observe a small difference between the flat surface (Cr=0) and other relative curvatures (approximately 7.2 % on average). Cr=0.2; i.e. the relative curvature with the lowest minor radius is the optimum case that satisfies the largest heat transfer rate beside the uniform heat transfer along the target surface (see Fig.3 and 4). These results correlate with the findings of other researchers (Fenot et al., 2008; Harrington et al., 2017; Patil and Vedula, 2018).

Figure 5 shows the comparison of pressure force coefficients for different relative curvatures (Cr). The pressure force coefficient decreases with increasing the relative curvature because the higher relative curvature which has a higher minor radius leads to the lower pressure on the curved surface.

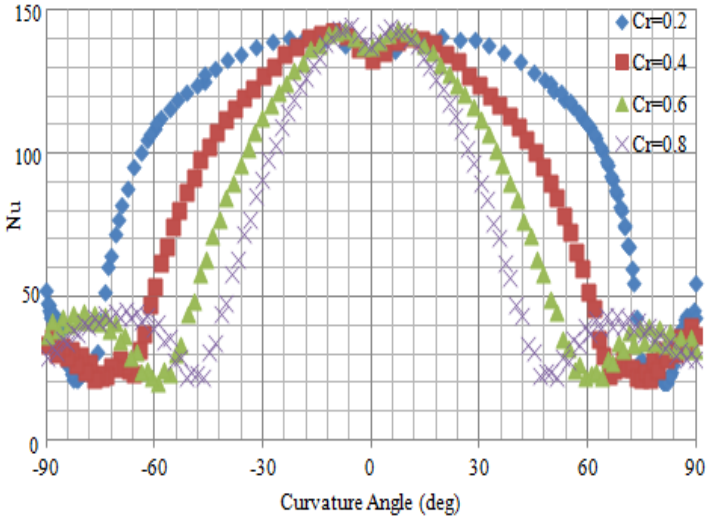

Fig. 3 Comparison the effect of relative curvature on the local Nu distributions along curvilinear axis on target plate from CFD (H/d=5, S/d=2, Re = 23000, VR=0)

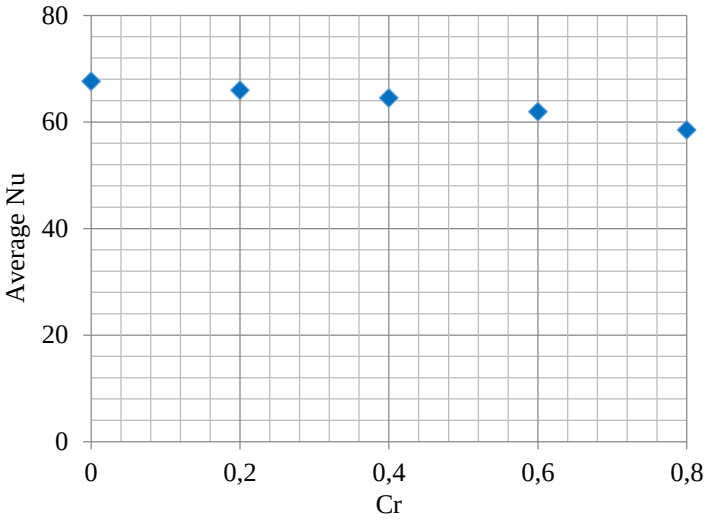

Fig. 4 Comparison of the effect of relative curvature on the total average Nusselt number on the target plate (H/d=5, S/d=2, Re = 23000, VR=0)

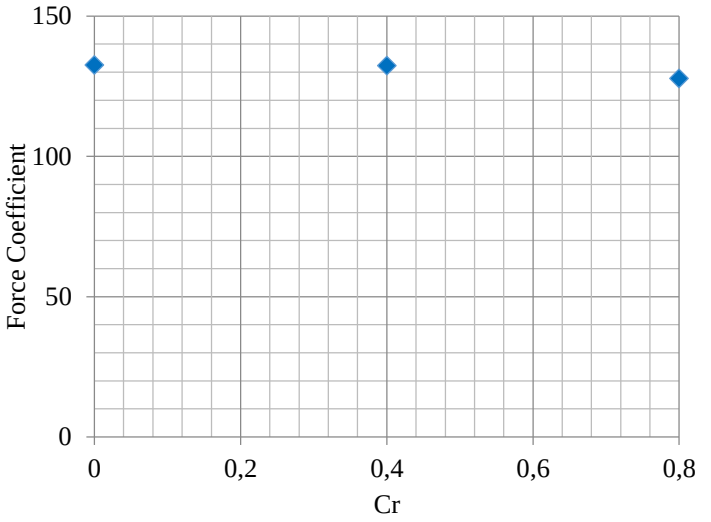

Fig. 5 Comparison of pressure force coefficient for different relative curvature at H/d=5, S/d=2, Re=23000, VR=0

3.3 Number of Jets

Sketch of the different configurations with the inline arrangement and variation of jet numbers are shown in Figure 6. The diameter of each round orifice (d) through a confinement plate with the length over the range of 120mm (3jets), 200mm (5jets), 280 mm (7jets), 520mm (13jets), 1000 mm(25 jets) and 1960mm(49 jets) is 10 mm. All configurations have the same array of 1 row with constant jet-to-jet distance S=4d and jet-to-plate distance H=5d.

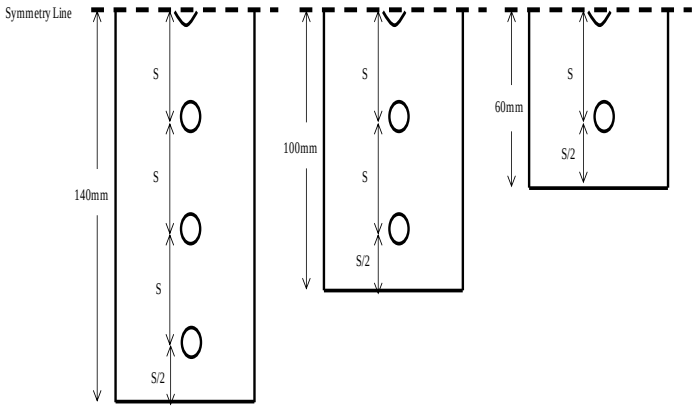

Fig. 6 Sketch of the different configurations with inline arrangement and variation of number of jets

The predicted Nusselt number distribution on the moving curved surface along the Z-axis for the multiple impinging jet system for the various number of jets or indeed for various lengths of jet rows is shown in Figure 7.

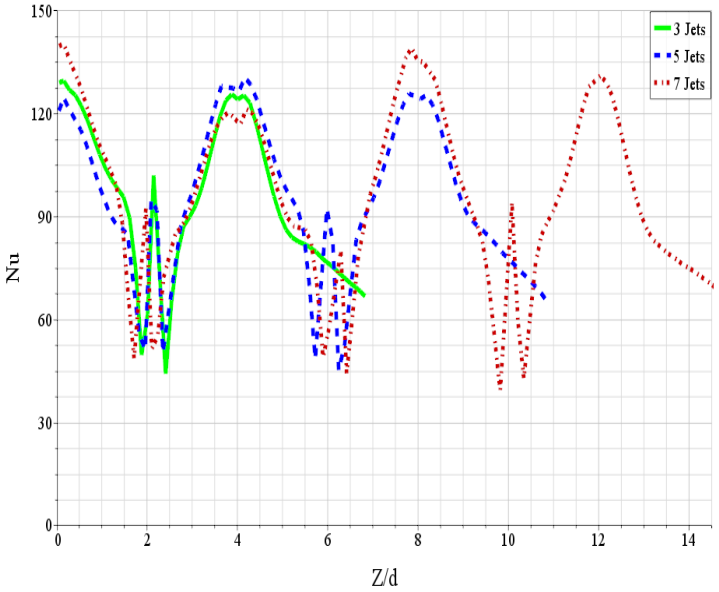

Fig. 7 Effects of number of jets on the local Nusselt number along Z-axis on the moving curved surface from CFD (inline arrays, Re=23000, H/d=5, S/d=4, Cr=0.8, and VR=0.28)

Figure 8 compares the effect of jet numbers on the total averaged Nusselt number on the moving curved surface. There is a minor difference in the total average Nu number and the maximum difference is around 2 %. For numerical simplification and in order to decrease the number of cells, three jets are considered for future investigations.

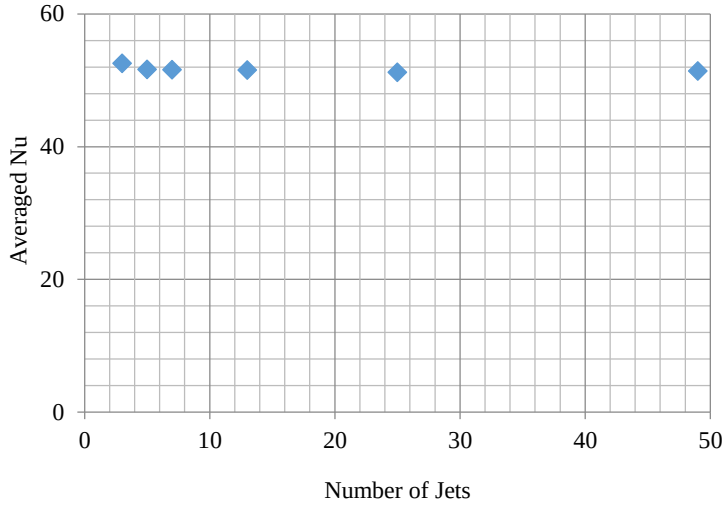

Fig. 8 Effects of number of jets on the total average Nusselt number on the moving curved surface (inline arrays, Re=23000, H/d=5, S/d=4, Cr=0.8, and VR=0.28)

3.4 Number of Jet Rows

Figure 9 shows the contour plot for local Nu distribution for single row inline and three-row inline configurations on the moving curved surface. For the single row case, the contours are seen to be stretching more in an outward chordwise direction due to jet to jet interaction in between two neighboring jets. However, for the three-row case, the stretching is uniform in both chordwise and spanwise directions. It is observed that the peak Nu values for three-row cases are noticed to be higher than single row cases. This slight difference is due to the much larger interaction of the three-row cases increasing the turbulence in the flow and thus improving the heat transfer at the stagnation region.

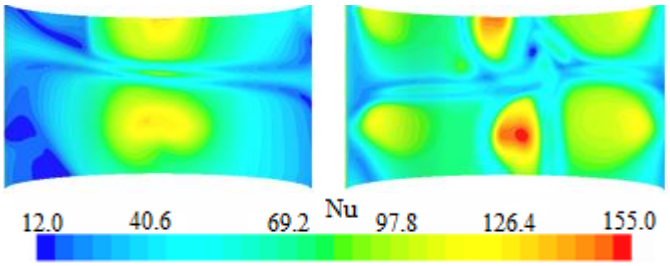

Fig. 9 Contour plots for single and multiple rows configurations on the moving curved surface (inline arrays, H/d=5, S/d=4, Cr=0.8, and VR=0.28)

Figure 10 shows the comparison of averaged Nu number along the Z-centerline (spanwise direction, the line passes the stagnation points) between single and multiple rows (3 rows) for inline arrays on the moving curved surface. The level of heat transfer for single rows is higher than the multiple rows by approximately 6%. This can attribute to the associated more powerful crossflow from multiple rows and surface motion, the heat transfer performance is considerably more dependent upon the number of rows on the moving surface (see Figure 9). Consequently, in terms of average heat transfer rates, increasing the number of rows degrade the performance. It was expected that the interaction might increase the turbulence in the flow and thus improve the heat transfer. However, the increase in the crossflow overweighs other changes. We observe the minor difference in the averaged Nu along Z-centerline between the single row and multiple rows. These results correlate with the findings of other researchers (Patil and Vedula, 2015; Bu et al. 2015).

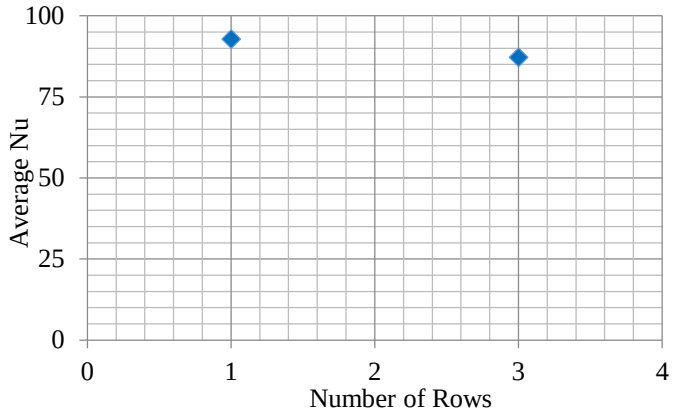

Fig. 10 Comparison of averaged Nu along Z-centerline between single and multiple rows (inline arrays, Re=23000, H/d=5, S/d=4, Cr=0.8, and VR=0.28)

3.5 Jet Arrangement

The arrays of jet arrangements are as shown in Figure 11 which depict the in-line configuration in (a) and the staggered arrangement in (b). The diameter d of each round orifice through a confinement plate of 120 mm length is 10 mm. Both jet arrangements have the same array of 1 row with 3 jet holes with constant jet-to-jet spacing S=4d and jet-to-plate distance H=5d. Note that due to symmetry, only half of the confinement plate is presented.

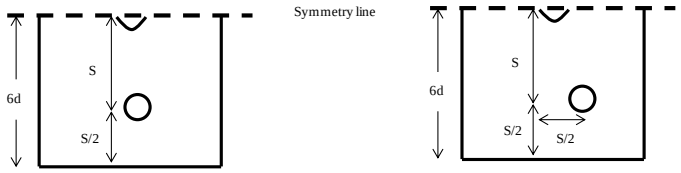

Fig. 11 Sketch of jet arrangement: (a) In-line arrangement and (b) staggered arrangement

The contours of the local Nusselt number on the moving flat and curved surface for the inline and staggered arrangements are shown in Figures 12 and 13.

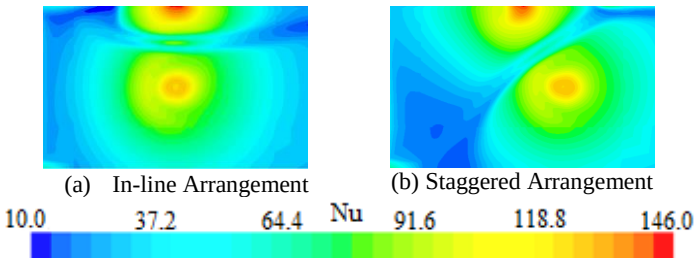

Fig. 12 Nusselt number distributions on the moving flat surface at Re=23000, H/d=5, S/d=4, Cr=0 and VR=0.28

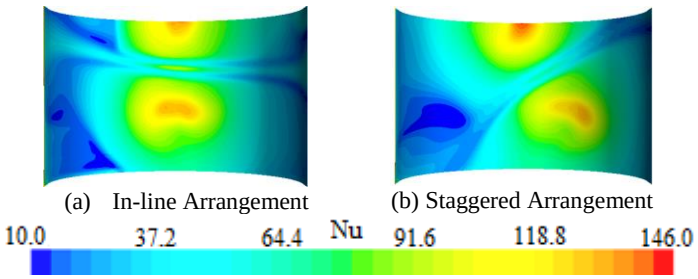

Fig. 13 Nu number distributions on the moving curved surface at Re=23000, H/d=5, S/d=4, Cr=0.8 and VR=0.28

It can be concluded from literature for fixed flat surfaces (Xing et al. 2010; Wae-hayee et al. 2013) that for the inline pattern the jets are protected from the oncoming crossflow by the upstream jets. For the staggered arrangement, the crossflow influences the jets more directly, which causes stronger diffusion and leads to a reduced overall heat transfer performance. We observe this trend for moving flat surfaces (see Figures 12 and 14). But this trend has a contrast with finding for moving curved surfaces. We can attribute this to the effect of surface curvature. Confinement is one effect of surface curvature and the staggered arrangement seems to decrease the effect of confinement (see Figure 3, 13, and 14). However, we observe a minor difference between inline and staggered arrangements on both moving flat and curved surfaces (see Figure 14). The inline arrangement has a more uniform heat transfer distribution compared to the staggered arrangement for both moving flat and curved surfaces. These results correlate with the findings of other researchers (Patil and Vedula, 2015).

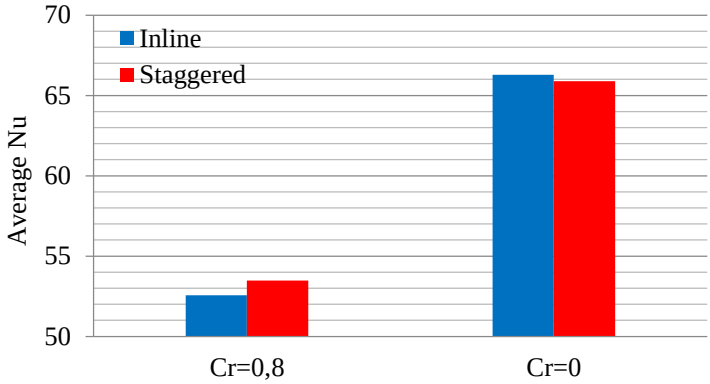

Fig. 14 Comparison of total average Nusselt numbers from CFD for different jet arrangements at H/d = 5, S/d=4, Re=23000 and VR=0.28

3.6 Cross Flow

In dryer application, we have two possibilities for boundary conditions on the front side of the dryer (see Figure 1). Selection of these boundary conditions which are either the adiabatic wall boundary condition (equivalent to the wall of computational domain coincides with sidewalls of the dryer) or the pressure outlet (equivalent to a sufficiently large gap between sheet and sidewall of the dryer) has dependency on the length of material being dried. It is very important to know how much the differences between both boundary conditions are. The contours of the local Nu number on the moving curved surface for both possible boundary conditions are shown in Figure 15.

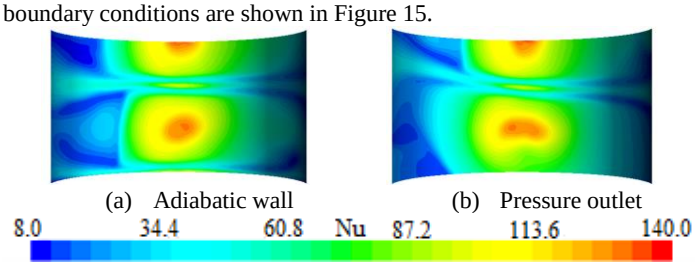

Fig. 15 Nusselt number distributions on the impingement surface for different boundary condition at Re=23000, H/d=5, S/d=4, Cr=0.8 and VR=0.28

If we impose the wall boundary condition or pressure outlet on the front side of geometry, we have the intermediate and minimum crossflow scheme respectively (see Figure 15). The crossflow is formed by the spent air of the jets and its strength is based on the outflow design. The jet flow in the wall boundary condition is more directed in direction of motion compared to the pressure outlet boundary condition. Therefore, the surface motion has a stronger effect on the impinging jets in the intermediate crossflow scheme than in the minimum crossflow scheme. The total average Nu number for boundary conditions as adiabatic wall and pressure outlet is 50.62 and 52.57 respectively and the maximum difference is approximately 3.5%. The best heat transfer performance with regard to the magnitude and uniformity occurs with the minimum

Global Digital Central
ISSN: 2151-8629

crossflow scheme. The intermediate and maximum crossflow conditions result in moderate and substantial reductions in the average heat transfer, respectively (Obot and Trabold, 1987). Thus, for further investigation, we consider the pressure outlet boundary condition on the front side of the dryer.

3.7 Surface Motion

Figure 16 compares the effect of velocity ratio of the moving plat to the jet velocity (VR) equal to 0, 0.0047(surface velocity=0.17), 0.047(surface velocity=1.7), and 0.28 (surface velocity=10) on the total average Nu number on the moving flat and curved surface.

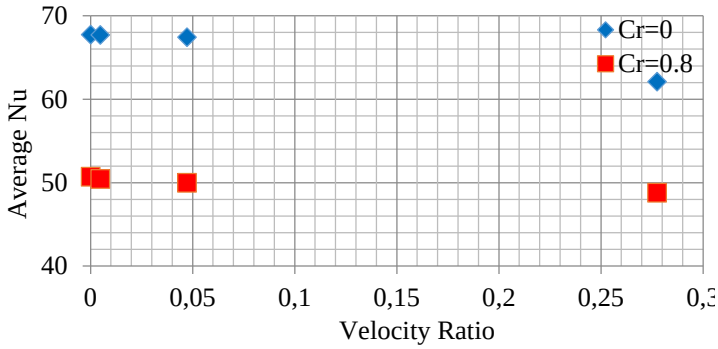

Fig. 16 Effects of velocity ratio on the total average Nusselt number on the moving flat and curved surfaces (inline arrays, H/d=2, S/d=4, Re=23000)

For a small velocity ratio (VR=0.005 and 0.05), the motion has little effect on the total averaged Nu number on both flat and curved surfaces. When the surface velocity is higher, the effect is like that of superposing a crossflow. It can be seen that the total averaged Nu on both flat and curved surfaces reduces with an increase in the velocity ratio. Thus, the moving surface reduces the effectiveness of each jet and the observed Nusselt number decreases from the surface motion effects become more pronounced as the velocity ratio increases. Other researchers (Chattopadhyay, 2006; Kadiyala and Chattopadhyay, 2017) confirm this observation for moving flat surfaces. The slope of averaged Nu number on the moving flat surface is sharper than the moving curved surface and the total averaged Nu number for the moving flat surface is higher than the moving curved surface. Both matters can be attributed to the effect of confinement. However, a higher velocity ratio helps to achieve a more uniform heat transfer distribution on both moving flat and curved surfaces (see Figures 17 and 18).

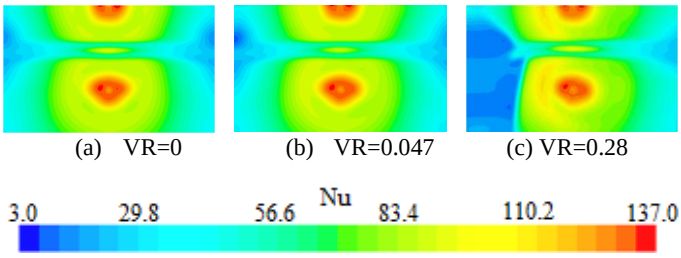

Fig. 17 Nusselt number distributions on the moving flat surface for different velocity ratio at Re=23000, H/d=2, S/d=4and Cr=0

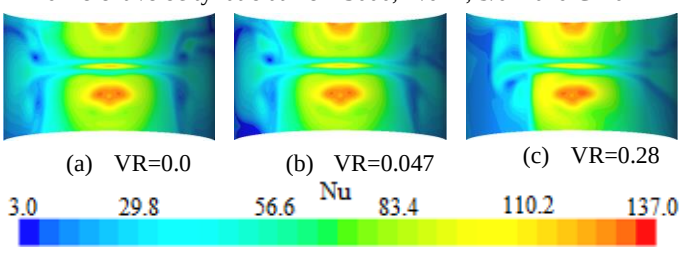

Fig. 18 Nusselt number distributions on the moving curved surface for different velocity ratio at Re=23000, H/d=2, S/d=4 and Cr=0.8

Figure 19 compares the effect of velocity ratio on the pressure force coefficient on the moving flat and curved surface. When the velocity ratio increases, the pressure force coefficient on the moving flat surface reduces due to the decrease in pressure on the moving flat surface. The variation of velocity ratio does not affect the moving curved surface. There is no significant difference in the pressure force coefficient between moving flat and curved surfaces. Thus, the pressure force is relatively insensitive to the surface motion on both flat and curved surfaces.

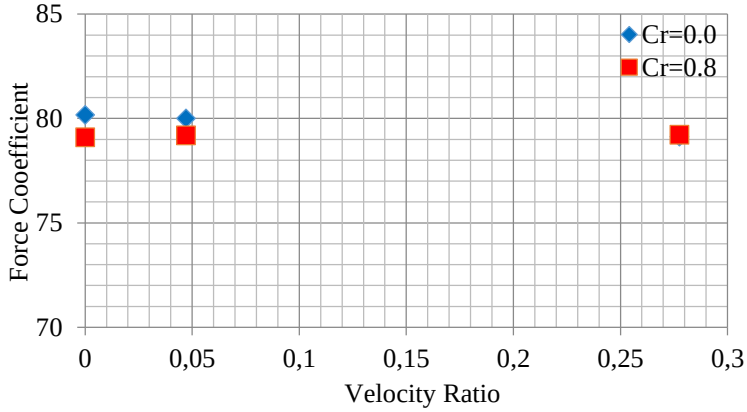

Fig. 19 Effects of velocity ratio on the pressure force coefficient on the moving flat and curved surface (inline arrays, H/d=2, S/d=4, and Re=23000)

4. Conclusion

Numerical simulations of multiple circular jets impinging on a fixed curved surface are carried out and validated against experimental data. The commercial CFD package STAR CCM+ is employed with the SST k−ω turbulence model. This article presents full CFD calculations of the heat transfer between multiple impinging circular jets and a moving curved surface. The effect of surface curvature, number of jets, number of jet rows, jet arrangement, crossflow, and surface motion on the heat transfer and pressure force has been evaluated. The results are as follows:

The surface curvature of the impingement plate produces a sort of confinement and reduces the average heat transfer and pressure force coefficients. The more number of jets has no significant effect on the average heat transfer rate. Increasing the number of rows degrades the average heat transfer rates, due to the associated more powerful crossflow. There is a minor difference between inline and staggered arrangements on both moving flat and curved surfaces. The inline arrangement has a more uniform heat transfer distribution compared to the staggered arrangement for both moving flat and curved surfaces. The surface motion has a stronger effect on the impinging jets in the intermediate crossflow scheme than in the minimum crossflow scheme. The total averaged Nu on both moving flat and curved surfaces reduces with an increase in the velocity ratio. The pressure force coefficient is relatively insensitive to the surface motion on both moving flat and curved surfaces.

NOMENCLATURE

A_f	open area ratio, total jet area to heat transfer area
A	surface area (m^2)
C_f	force coefficient
d	jet diameter (m)
F	force (N)
H	nozzle-to-target spacing (m)
k_t	thermal conductivity (W/m·K)
Nu	Nusselt number
P	pressure (pa)
q	convective heat flux (W/m^2)

Global Digital Central
ISSN: 2151-8629

R_1	Minor curvature radius (m)
R_2	Major curvature radius (m)
Re	Reynolds number (Re=Vd/ν)
S	jet pitch (m)
S_x	streamwise jet-to-jet distances (m)
S_y	spanwise jet-to-jet distances (m)
T	temperature (K)
V	magnitude of jet exit velocity (m/s)
y+	dimensionless wall distance

Greek letters

k	turbulence kinetic energy (kgm^2/s^2)
ω	specific dissipation rate of turbulence kinetic energy (1/s)
θ	jet inclined angle with respect to the horizontal axes (°)
ρ	density of the fluid (kg/m^3)
ν	kinematic viscosity (m^2/s)

Subscripts

ave: average
j: jet
w: wall

Abbreviation

Cr: curvature ratio; the ratio of minor to the major radius
CFD: computational fluid dynamic
GCI: grid convergence index
VR: velocity ratio; surface to jet velocity
SST: shear stress transport

Reference

Bu X., Peng L., Lin G. et al. (2 more authors), 2015, "Experimental study of jet impingement heat transfer on a variable-curvature concave surface in a wing leading edge," J. Heat and Mass Transfer, 90, 92-101. https://doi.org/10.1016/j.ijheatmasstransfer.2015.06.028

Chattopadhyay H., 2006, "Effect of surface motion on transport processes due to circular impinging jets – a numerical study," *J. Drying Technology*, 24(11), 1347-1351. https://doi.org/10.1080/07373930600951117

Chitsazan, A., Glasmacher, B., 2020, "Numerical investigation of heat transfer and pressure force from multiple jets impinging on a moving flat surface," *Int. J. Heat and Technology*, 38, 601-610. https://doi.org/10.18280/ijht.380304

Fenot, M., Dorignac E., Vullierme J.-J.,2008, "An experimental study on hot round jets impinging a concave surface," *J. Heat and Fluid Flow*, 29(4), 945–956. https://doi.org/10.1016/j.ijheatfluidflow.2008.03.015

Harrington J., Hossain J., Wang W. et al. (3 more authors), 2017, "Effect of target wall curvature on heat transfer and pressure loss from jet array impingement," *J. Turbomachinery*, 139(5), 051004-051004-13. https://doi.org/10.1115/1.4035160

Kadiyala P.K., Chattopadhyay H., 2017, "Numerical simulation of transport phenomena due to array of round jets impinging on hot moving surface," *J. Drying Technology*, 35(14), 1742-1754. https://doi.org/10.1080/07373937.2016.1275672

Li, X. C., and Corder, P., 2008, "Characteristics of cooling of the leading edge with a row of dual impinging jets," *ASME Paper No. HT2008-56347*. https://doi.org/10.1115/HT2008-56347

Obot N. T.and Trabold T. A., 1987, "Impingement heat Transfer within arrays of circular jets: Part 1- effects of minimum, intermediate, and complete Crossflow for small and large spacings," *J. Heat Transfer*, 109(4), 872-879. https://doi.org/10.1115/1.3248197

Patil V. S. and Vedula R. P., 2015, "Heat transfer with single and two rows of axisymmetric jets impinging on a concave surface," *1st International ISHMT-ASTFE Heat and Mass Transfer Conference*, Thiruvananthapuram, India.

Patil V. S. and Vedula R. P., 2018, "Local heat transfer for jet impingement on a concave surface including injection nozzle length to diameter and curvature ratio effects," J. Experimental Thermal and Fluid Science, 92, 375-389. https://doi.org/10.1016/j.expthermflusci.2017.08.002

Roache, P. J., 2003, "Conservatism of the grid convergence index in finite volume computations on steady-state fluid flow and heat transfer," *J. Fluids Engineering*, 125, 731–735. https://doi.org/10.1115/1.1588692

Wae-hayee, M., Tekasakul, P., & Nuntadusit, C., 2013, "Influence of nozzle arrangement on flow and heat transfer characteristics of arrays of circular impinging jets," *J. Science & Technology*, 35(2), 203-212.

Xing, Y., Spring, S., and Weigand, B., 2010, "Experimental and numerical investigation of heat transfer characteristics of inline and staggered arrays of impinging jets," *J. Heat Transfer*, 132(9), 092201. https://doi.org/10.1115/1.4001633

Zuckerman, N. and Lior, N., 2006, "Jet impingement heat transfer: physics, correlations, and numerical modeling," *J. Advances in heat transfer*, 39, 565-631. https://doi.org/10.1016/S0065-2717(06)39006-5